CREEP OF A UNIAXIAL METAL MATRIX COMPOSITE SUBJECTED TO AXIAL AND NORMAL LATERAL LOADS

T.R. BRANCA, A.P. BORESI,

Department of Theoretical and Applied Mechanics,
University of Illinois, Urbana, Illinois, U.S.A.

ABSTRACT

A displacement formulation of the finite element method is used to solve the generalized plane strain problem of the creep of a uniaxial metal matrix composite subjected to axial load and normal lateral loads. Inelastic strains are considered as initial strains in the finite element analysis. The composite is examined from a micromechanical point of view. Particular boundary conditions resulting from rectangular close-packed filament spacing are included in the analysis.

For the special case of no lateral loads, analytical predictions are compared to experimental results for a composite of copper wires embedded in a lead-tin alloy matrix.

The finite element method provides an efficient solution to this problem. Analytical results so obtained agree well with experimental results. Furthermore, for sample cases of zero lateral loads, axial strain of the composite as predicted by the finite element method agrees well with a composite mixing-law prediction.

Analytical results are also given for a silicon-carbide titanium composite subjected to axial and lateral load combinations. For this composite system under axial loading (zero applied lateral loads), the mixing-law solution is again adequate to predict the axial strain; however, it is shown that lateral interaction has a significant influence on the stress state within the matrix of the composite.

INTRODUCTION

With the increasing number of high temperature applications of metal matrix composites, it is of interest to examine the creep of these materials. In particular, this study presents a micromechanical solution for creep of a uniaxial, continuously reinforced, metal matrix composite. The composite is subjected to constant axial and normal lateral loads at constant temperature.

The analysis is greatly simplified if the following assumptions are made. First, the region of the composite member investigated is sufficiently far from loading regions so that axial components of shearing stress at the fiber matrix interface are negligible. Second, in the cross-section the fibers are taken to be positioned in a regular, rectangular array. Third, the component materials of the composite are taken to be isotropic and homogeneous throughout the loading process.

The first and second assumptions lead to the condition of generalized or modified plane strain. For this state in uniaxial reinforced composites, the non-zero stresses consist of normal stress in the fiber direction, normal stresses in the lateral directions, and shear stress in the lateral plane. The strain in the axial direction is not assumed but is considered unknown.

One-Dimensional or Mixing-Law Analyses. If there are no applied lateral loads, the important special case of the uniaxial composite under axial loading results. Furthermore, if stresses developed by the lateral interaction between the fiber and matrix are considered small, a one-dimensional state of stress is assumed to exist. Under these conditions the axial stresses and creep strains may be predicted by an analysis based on a composite mixing-law. This mixing-law analysis has been used to determine steady-state creep response of uniaxial composites [1-4]. Ellison and Landes [5] have used a mixing-law solution to determine the primary response of a metal-matrix system. Antans and Skudra [6] have used a viscoelastic material description, in conjunction with the mixing-law, to obtain a solution for the axially-loaded reinforced plastic material. Axial creep of a short fiber composite has been considered by deSilva [7].

Analyses which Consider Lateral Stresses. Because of good agreement with experiments, the mixing-law analyses serve as indications that the assumption of a one-dimensional stress state is probably valid for the axially loaded, uniaxial composite. Nevertheless, in complicated load and temperature histories, a truer representation of the state of stress, which includes the effect of lateral stresses, is required, even for the axial loading case.

To solve the more general problem where stress due to lateral interaction is not ignored, investigators have used finite element methods. Owen, Holbeche, and Zienkiewicz [8] consider the plane problem of a short fiber interacting with neighboring fibers through an inelastic matrix. They also consider the axisymmetric problem of a short fiber embedded in a cylinder of inelastic material. Adams [9], in a study of inelastic deformation of a unidirectional composite subjected to normal lateral loads, suggests a modification of his method to include axial and normal lateral loads. However, to incorporate plastic strains, Adams employs a technique which requires inversion of the matrix of the finite element equations for each plastic strain change. For the iteration scheme used in the present study, Adams' method would be extremely expensive from the view point of computer execution time. A more efficient analysis is presented by Isakson [10], who considers plastic strains as initial strains, separate from elastic properties of the system. The virtues of this approach are discussed by Greenbaum and Rubenstein [11]. In the present study, a method is developed to incorporate boundary conditions resulting from the constraint of rectangular fiber spacing and from the constraint of the generalized plane strain state. The same technique is applicable to both types of constraint. This advantage does not seem possible using Isakson's technique. For the particular problem being considered, the present method appears to be more unified, but not necessarily more efficient, than Isakson's.

Even with the available analyses cited, there is a need to investigate the particular inelastic problem of metallic creep. With the present study, it is hoped that the reader can obtain a better understanding of the relative importance of the fiber-matrix interactions within a creeping uniaxial composite.

ANALYSIS

Idealization of the Composite. Composite Repeating Unit. Since only regular, rectangular filament spacing in the composite cross-section is considered, we may divide the composite cross-section into identical basic cells or repeating units as shown in fig. (1). Because of the rectangular spacing, the stress states and strain states of every cell are identical. Accordingly, if the stress and strain states for one unit or by symmetry one quarter of a unit are found, the stress and strain states for the entire composite cross-section are determined.

To study the boundary value problem of a basic cell, we must replace the effects of contiguous cells by appropriate boundary conditions. Piehler [12] gives an extensive discussion of these boundary conditions. For the rectangular unit considered in this analysis, appropriate boundary conditions are listed in fig. (2). We note that conditions which cause particular difficulty in the finite element idealization are those due to the restriction that the cell surface $z = 1$ remain plane and normal to the z-axis and the restrictions that surfaces $x=a$ and $y=b$ remain normal to x and y axes, respectively. In the present study, the generalized plane strain constraint is satisfied by selecting an element for the finite element analysis that is consistent with this constraint.

Element Stiffness. Since it is possible for the composite to deform in the axial direction, we include in the finite element idealization a degree of freedom in the z-direction. Therefore, in addition to the triangular plane strain element with linear varying strain (nodes at mid-points of the sides), a nodal displacement is included in the z-direction, fig. (3). The displacement functions for the element are

$$\begin{aligned} u(x,y) &= A_1 + A_2x + A_3y + A_4x^2 + A_5xy + A_6y^2 \\ v(x,y) &= A_7 + A_8x + A_9y + A_{10}x^2 + A_{11}xy + A_{12}y^2 \\ w(z) &= A_{13}z \end{aligned} \tag{1}$$

Since the surface $z=1$ of the element is restricted to remain normal to the z-axis, only one nodal z-displacement is required.

For small strains, the strain-displacement relations are

$$\varepsilon_x = \frac{\partial u}{\partial x},\ \varepsilon_y = \frac{\partial v}{\partial y},\ \ \varepsilon_z = \frac{\partial w}{\partial z},\ \ \gamma_{xy} = \left(\frac{\partial u}{\partial y} + \frac{\partial v}{\partial x}\right) \tag{2}$$

where the strain components ε_x, ε_y, ε_z, γ_{xy} consist of elastic components ε_x^E, ε_y^E, ε_z^E, γ_{xy}^E and inelastic or creep components ε_x^c, ε_y^c, ε_z^c, γ_{xy}^c. Thus, we have

$$\begin{Bmatrix} \epsilon_x \\ \epsilon_y \\ \epsilon_z \\ \gamma_{xy} \end{Bmatrix} = \begin{Bmatrix} \epsilon_x^E + \epsilon_x^c \\ \epsilon_y^E + \epsilon_y^c \\ \epsilon_z^E + \epsilon_z^c \\ \gamma_{xy}^E + \gamma_{xy}^c \end{Bmatrix} \tag{3}$$

Solving eq. (3) for the elastic strains $\epsilon_x^E = \epsilon_x - \epsilon_x^c$, etc., we may write Hooke's law for an isotropic material in the form

$$\{\sigma\} = \frac{E}{(1+\nu)(1-2\nu)} \begin{bmatrix} 1-\nu & \nu & \nu & 0 \\ \nu & 1-\nu & \nu & 0 \\ \nu & \nu & 1-\nu & 0 \\ 0 & 0 & 0 & \frac{1-2\nu}{2} \end{bmatrix} \{\epsilon\} - 2G\{\epsilon^c\}$$

or

$$\{\sigma\} = [D]\{\epsilon\} - 2G\{\epsilon^c\} \tag{4}$$

where $\{\sigma\} = [\sigma_x, \sigma_y, \sigma_z, \tau_{xy}]^T$ is the stress vector, $[D]$ is the elasticity matrix, $\{\epsilon\} = [\epsilon_x, \epsilon_y, \epsilon_z, \gamma_{xy}]^T$ is the strain vector and $\{\epsilon^c\} = [\epsilon_x^c, \epsilon_y^c, \epsilon_z^c, \frac{1}{2}\gamma_{xy}^c]^T$ is the creep strain vector. In eq. (4), we have employed the condition that $\epsilon_x^c + \epsilon_y^c + \epsilon_z^c = 0$, i.e., that this inelastic (creep) deformation is incompressible.

To be consistent with the assumed displacement functions eq. 1, the creep strains must vary in a linear manner within an element. Thus

$$\{\epsilon^c\} = [a] \begin{Bmatrix} 1 \\ x \\ y \end{Bmatrix} \tag{5}$$

The elements of matrix $[a]$ are defined once a set of creep strains is selected for the corners of the finite element.

With eqs. (1) and (2), the strains may be related to the nodal displacements for an element in the form

$$\{\epsilon\} = [B]\{u\} \tag{6}$$

where $[B]$ is a known matrix and $\{u\}$ is the nodal displacement vector. The equilibrium nodal displacements which result from a given set of initial creep strains and a set of known applied forces on the element may be determined by the principle of virtual work. The result is:

$$\{f\} = \int_V [B]^T [D] [B] \, dV \{u\} - 2G \int_V [B]^T [a] \begin{Bmatrix} 1 \\ x \\ y \end{Bmatrix} dV \tag{7}$$

where $\{f\}$ is the vector of applied nodal forces.

After integration over the element volume, eq. (7) may be written

$$[k] \ \{u\} = \{f\} + \{f^c\} \qquad (8)$$

where $[k]$ is the element stiffness matrix and the vector $\{f^c\}$ represents psuedo forces which, when applied to the element, yield the creep strains selected for eq. (5); $\{f^c\}$ is thus called the "creep force" vector.

Finite Element Idealization of the Repeating Cell. The composite is idealized by an assemblage of finite elements. A grid system that is used to model one of the units (cells) is shown in fig. (4). By superimposing the element stiffnesses, we obtain the total stiffness matrix of the system. The equations among all nodal displacements of the grid are expressed by the usual relation

$$[K] \ \{U\} = \{F\} + \{F^c\} \qquad (9)$$

Each element has one nodal displacement in the z-direction. However, because of the generalized plane strain constraint there is only one z-displacement for the entire composite unit. Therefore, only one z-displacement unknown, w, is included in the vector of unknowns, $\{U\}$. Letting the last entry in $\{U\}$ be w, we obtain an unusual form for the total stiffness matrix. Since every nodal displacement is directly influenced by w, each equation among the displacements varies from its usual banded character to include a term involving w. The matrix $[K]$ however, is symmetric. A schematic representation of the system of equations is given in fig. (5). By superposition to obtain $[K]$, the components of $\{F\}$ and $\{F^c\}$, corresponding to w, are the total applied force in the z-direction and the total "creep force" in the z-direction.

Essentially the same technique is used to include the displacement constraints on the composite cell faces $x=a$ and $y=b$. The face $x=a$ is constrained to remain perpendicular to the x-axis. Therefore, all x-displacements of that face must be equal. Similar considerations hold for the y-displacements on the face $y=b$. Thus, the vector $\{U\}$ has redundant displacement entries. It is desirable to eliminate redundant nodal displacement unknowns from the assembled equations without disrupting more than necessary the symmetry or banded qualities of the equations.

For convenience, the upper-right-corner node of the composite unit grid is given the largest node number. The x and y-displacement components (u,v) of that node therefore appear just above the z-displacement in $\{U\}$. They are unknowns $N-2$ for u and $N-1$ for v where the total number of equations is N. Consider the x-direction. The procedure to eliminate redundant unknowns consists in collecting all stiffnesses and forces corresponding to the u unknowns into one equation as was done for w. To accomplish this, each equation with a redundant u component on the main diagonal is added to the equation $N-2$. To preserve the symmetry, the columns of $[K]$ corresponding to the u components of the face $x=a$ are each added to column $N-2$. Now, except for the (N-2)nd row and column, the rows and columns of the unknowns involved have been eliminated from the matrix [K]. The size of the stiffness matrix is thus reduced by the number of nodes on the face $x=a$ less one. A similar procedure is used to incorporate the constraint of the face $y=b$. The two remaining unknowns involved in these displacement constraints, designated as u_a and v_b, now appear in the system of equations as shown in fig. (5). These two equations violate the band width of the other equations. As with the z-displacement unknown, the forces associated with u_a and v_b are simply the total externally applied forces and the total "creep forces" on the corresponding faces. The remaining displacement boundary conditions on the composite unit are incorporated as in the usual finite element method.

Unfortunately, due to limitations of computer storage and execution time, the numerical solution is a more difficult problem than the preceding analysis would indicate. These difficulties are related to the manner in which the total stiffness matrix must be stored for efficient calculations. If the total stiffness matrix is stored as a full matrix, as shown in fig. (5), an intolerable number of zeros must be stored. Furthermore, even if the zeros are stored successfully, machine operation on zeros in the computer solution results in prohibitive machine time. The usual remedy for these difficulties is to take into account the symmetric banded properties of the matrix and store only terms on or above the main diagonal that fall within the band limit. However, in the present problem, the three troublesome equations corresponding to u_a, v_b and w violate the band width and must be considered as full equations. It is therefore necessary to store these three equations as full and the remaining equations as banded. This remedy requires a special equation solver and a great deal of "bookkeeping" to obtain a solution.

Description of Material Properties. The creep properties of the component materials of the composite are introduced into the finite element solution through the "creep force" vector of eq. (9). For this purpose, we assume that the Prandtl-Reuss equations of plasticity theory predict the increments of creep strain necessary to calculate $\{F^c\}$. Thus, for the increments of creep strains we write

$$\Delta\varepsilon_{ij}^c = \frac{3}{2}\frac{\Delta\varepsilon_e^c}{\sigma_e} S_{ij} \tag{10}$$

where $\Delta\varepsilon_e^c$ is the equivalent creep strain increment given by

$$\Delta\varepsilon_e^c = \frac{\sqrt{2}}{3}[(\Delta\varepsilon_x^c - \Delta\varepsilon_y^c)^2 + (\Delta\varepsilon_y^c - \Delta\varepsilon_z^c)^2 + (\Delta\varepsilon_z^c - \Delta\varepsilon_x^c)^2 + 6(\Delta\varepsilon_{xy}^c)^2]^{1/2} \tag{11}$$

σ_e is the equivalent stress given by

$$\sigma_e = \frac{1}{\sqrt{2}}[(\sigma_x-\sigma_y)^2 + (\sigma_y-\sigma_z)^2 + (\sigma_z-\sigma_x)^2 + 6\sigma_{xy}^2]^{1/2} \tag{12}$$

$\Delta\varepsilon_{ij}^c$ and S_{ij} are the tensor of creep strain increments and the stress deviator tensor, respectively. ε_e^c the equivalent creep strain is given by

$$\varepsilon_e^c = \frac{\sqrt{2}}{3} [(\varepsilon_x^c - \varepsilon_y^c)^2 + (\varepsilon_y^c - \varepsilon_z^c)^2 + (\varepsilon_z^c - \varepsilon_x^c)^2 + 6{\varepsilon_{xy}^c}^2]^{1/2} \tag{13}$$

With this formulation, all creep properties that are needed are obtained from uniaxial creep curves. By eq. (12) and (13) the equivalent stress and strain properties may be computed directly. The component material creep curves are approximated by an appropriate empirical expression. For example Garofalo [13], suggests the relation

$$\varepsilon^c = A(\sinh b\sigma)^m \, t^n \tag{14}$$

where A, b, m and n are empirically determined parameters. According to Garofalo, the hyperbolic sine function of stress gives an accurate fit to the creep curves over a large range of stress. The parameters A, b, m and n may be determined by a least squares curve-fitting technique described by Conway [14].

Creep Iteration Scheme. To develop the time dependent solution for creep, the method of successive elastic solutions as described by Mendelson, et al. [15,16], is used. A brief description of the method as applied in the present study follows.

(1) An estimate is made of the creep strain increments that take place over a time increment Δt. The creep strains and stresses are calculated for corners of the elements. Therefore, it is necessary to estimate the creep increments at each element corner.

(2) With this set of creep strains, the "creep force" vector, as described in eqs. (7), (8), and (9) is calculated.

(3) After upper-triangularizing the total stiffness matrix of eq. (9), the first set of nodal displacements and subsequent sets, are obtained by back-substitution. The stresses at the element corners are next calculated and used as input to eq. (10).

(4) The equivalent creep strain increment $\Delta\varepsilon_e^c$ (eq. 10) is calculated by substituting the estimates of the creep strain increments in eq. (11).

(5) To determine the equivalent stress σ_e, the empirical relation, eq. (14), is converted to an incremental strain hardening relationship between the equivalent stress and strain in the form

$$\Delta\varepsilon_e^c = f(\sigma_e, \varepsilon_e^c)\Delta t \tag{15}$$

With the estimated creep strain increments, eq. (15) is used to determine σ_e.

(6) With the right hand side of eq. (10) known, new estimates of the creep strain increments may be determined for the time interval Δt.

(7) The improved creep strain estimates are then compared to the estimates assumed at the start of the cycle. If they do not agree to within some pre-set tolerance, the cycle is repeated using the improved estimates of the creep strain increments as new initial guesses.

(8) When convergence is obtained to within acceptable tolerance, the accumulated creep strain and total time are established. The increments of creep strain at convergence are then used as the initial estimates for the next time step.

To accelerate the convergence, every fourth estimate of the creep strain increments is determined by a process called "extrapolation to zero difference" [16] (or Atkin's δ^2 process). The process determines the fourth estimate for $\Delta\epsilon_{ij}^{c}$ by using the preceding three estimates to extrapolate to a point indicating zero difference between successive estimates.

To accelerate the iteration, the length of the time step was varied in the calculations. A very small step is required for early times during which the creep is changing rapidly. Initially, a relatively large number of iterations is needed to obtain convergence. However, as time proceeds, the slopes of the creep strain vs time curves decrease. This effect is coupled with improvement in initial guesses for creep increments. The net result is that the number of iterations necessary for convergence decreases as the solution advances in time. To improve the efficiency of the successive elastic solution iteration, when the number of iterations required for convergence decreases below a specified level, the length of the next time increment may be increased over the last step. In this study a ten percent increase was very satisfactory.

EXPERIMENTAL PROCEDURE

To check the solution, the special case of axial load with zero applied lateral loads was investigated experimentally. Difficulties reported in the literature related to the composite creep test such as the control of the component materials in composite form and individually, the gripping of the composite, the fiber alignment and cross-sectional spacing, and obtaining measurable axial creep were to a large part eliminated by experimenting at room temperature with a model system consisting of 0.010 in. dia. copper wires embedded in a lead-tin (Pb-Sn) alloy matrix. The wires were commercial tough-pitch copper, and the matrix material was commercial solder, 40% by weight lead.

The fabrication of the composites was accomplished by first straightening the wire and then winding it around a metal frame, the spacing between the wires being controlled by a lathe feed. Small tabs were next cemented to the ends of the wires, fig. (6). The tabs held the wire in place when it was removed from the frame. The wire mats which resulted were next stacked and positioned within an aluminum mold. After cleaning the wires and pre-heating the mold, the molten matrix material was cast around the wires. The resulting composite cross-section for 14.2% fiber is shown in fig. (7). The reduced section of the composite test specimens had cross-sectional dimensions of 0.625 in. by 0.375 in. and was 3.5 in. in length.

The wire properties were determined by testing individual wires which had been straightened and heat treated in a manner duplicating as closely as possible the heat cycle of the fabrication process. The elongation in a 10 in. gage length was measured by a linear variable differential transformer. The creep curves for the copper wires along with the empirical fit of eq. (14) are given in fig. (8). The blanks of the matrix material were cast in the same mold as the composite specimens. Deformation of the matrix and composite specimens was monitored by a wire resistance, clip extensometer. Experimental creep and empirical curves for the matrix material are given in fig. (9).

The creep data for the titanium matrix material of the silicon-carbon titanium (SiC-Ti) composite system studied, is that of Sidebottom [17]. The data is reproduced in fig. (10). The SiC reinforcing is assumed to remain elastic. The elastic and creep properties of the materials used are given in table (1).

RESULTS AND DISCUSSION

For the 335 unknowns (with band width 90) of the element grid shown in fig. (4), the technique described to incorporate the constraints of the generalized plane strain and the constraints of the lateral boundary conditions make an in-core, double precision solution possible on the IBM 360/75. For this system of equations, approximately 20 sec. was required to execute the first cycle of the creep iteration and less than 3 sec. for each cycle thereafter.

The rate of convergence is dependent on the definition of convergence. The results presented here were calculated subject to the convergence requirement that the improved estimates for the creep strain increments for each corner of each element were to differ from the last estimates by less than the relative amount of 0.5% for the axial creep strain increments and 1.0% for the other increments. During the early stages of the creep solution, ten to twenty cycles were required to obtain convergence. The later stages of the solution required only two or three cycles for convergence. In general, for cases with applied lateral loads, the number of cycles for convergence is slightly greater than for the zero lateral load cases.

The "extrapolation to zero difference" reduced the number of iterations necessary for convergence by at least a factor of two. Ten percent increase in time step size also helped convergence. This improvement was probably due to the improvement in the initial estimates for $\Delta\varepsilon^c_{ij}$ at a given time step. The improvement is due to the favorable interaction between the decreasing slope of the component creep curves and the increased step size. Time increments at the start of the solution were taken as 0.001 hr. At the end of the solution, five hours of creep data, the time increments had increased to approximately 0.5 hr.

The experimental and analytical results for axial loading of the Cu-(Pb-Sn) composite are given in fig. (11). In contrast to the good agreement between theory and experiment for the 4 ksi load, the 3 ksi and the 5 ksi experiments deviate from the theory. In the 3 ksi case, the deviation is believed due to the failure to consider creep recovery in the hardening scheme. The deviation in the 5 ksi case is due mainly to the fact that the load on the wire reinforcement exceeds the range in which the properties for the copper were defined. The analytically predicted axial stress in the copper after 0.5 hr. is 29.2 ksi. This is well above the stress levels considered for copper in fig. (8).

In fig. (11), the analytical predictions from the analysis based on the composite mixing-law are in close agreement with the finite element solution. This result indicates that either the effect of the lateral interaction averages out or that the lateral interaction quickly diminishes to zero. The latter is seen to be the case by fig. 12. In fig. (12) it may also be noted that the stress boundary condition on the face $x=a$ given in fig. 2 is satisfied.

The conditions which lead to the lack of importance of the lateral stresses are first, the low density of the filaments for the composite considered, and second, the inability of the matrix material to support large stresses. The varying Poisson's ratios of the component materials also contribute to the smallness and rapid decay of the lateral stresses. With plastic strain, the Poisson ratios of both component materials tend towards 0.5. Since the ratios are converging toward each other, the tendency for lateral interaction decreases with creep. The rapid decay of the lateral stresses was also found in a composite of 62.1% copper.

In a creeping composite material where the fiber remains elastic this convergence of the Poisson's ratios does not occur. The axial loading of a SiC-Ti composite was investigated analytically to study this effect. The contours for stress σ_x, fig. (13), show that the lateral stress is intensified by the creep. It does not, however, become very large in relation to the 160 ksi axial stress on the composite. The axial strain ε_z as predicted from the mixing-law analysis and as predicted from the finite element analysis are in close agreement.

A study of the axial stress σ_z in the cross-section, fig. (13), reveals that axial compression is developed in the matrix of the composite loaded axially in tension. For the case of cyclic creep loading on such a composite there would be a stress amplification effect within parts of the matrix. This amplification could strongly influence the fatigue and fracture properties of the composite.

Analytical results for a non-zero lateral load case, $\bar{\sigma}_x = -15$ ksi, on the silicon-carbide titanium composite are given in fig. (14). We see that the stress concentrations are intensified with creep.

A more detailed discussion of the topics of this paper appear in ref. (18).

Conculsions

1. The method described to incorporate the axial and lateral constraints into the finite element method provides a direct and efficient means to solve for the complete set of stresses and strains in a creeping uniaxial metal matrix composite subjected to axial and normal lateral loads. More complete material descriptions are needed to improve the solution and to make possible the inclusion of epoxy matrix materials.
2. The Cu-(Pb-Sn) composite was found relatively easy to fabricate and test and thus provides a suitable system for creep studies.

3. For the composites studied, consideration of the lateral interaction in the axial loading case (no laterally applied forces) did not significantly change the prediction for axial strain from that of a one-dimensional creep analysis.
4. For the elastic fiber plastic matrix case studied, the lateral stresses intensified with creep. The lateral stresses did not become large relative to the applied axial load, but their influence on the state of stress within the composite is significant.

ACKNOWLEDGMENT

The authors are indebted to the graduate students and staff of the Department of Theoretical and Applied Mechanics, University of Illinois, who have been both stimulating and encouraging during this research.

Financial support for the first author has been provided by the Atomic Energy Commission in the form of a Special Fellowship in Nuclear Science and Engineering and by a contract from Naval Air System Command (Contract No. N00019-70-C-0231). The work was also supported in part by NSF Grant Number GK-13613.

TABLE 1. CREEP AND ELASTIC MATERIAL PROPERTIES

				Coefficients of eq. 14			
Material	T(°F)	E(ksi)	ν	A	b	m	n
Cu	74	16,000	0.33	0.001598	0.03	2.60	0.102
Pb-Sn	74	4,855	0.43	0.03391	0.24	1.90	0.585
SiC	1000	70,000	0.24	---	---	---	---
Ti 6Al-4V	1000	11,500	0.34	0.000582	0.16	0.92	0.591

Bibliography

1. McDanels, D. L., Signorelli, R. A., and Weeton, J. W., "Analysis of Stress-Rupture and Creep Properties of Tungsten Fiber Reinforced Copper Composites," Fiber Strengthened Metallic Composites, A.S.T.M. STP 427 (1967), pp. 124-148.

2. Antony, K. C., and Chang, W. H., "Mechanical Properties of Al-B Composites," Transactions of the ASM, vol. 61, (1968), pp. 550-558.

3. Wilcox, B. A., and Clauer, A. H., "Tensile and Creep Deformation of a Fiber Reinforced Mg-Li Alloy," Transactions of the Metallurgical Society of AIME, vol. 245, (May 1969), pp. 935-939.

4. Hayashi, Tsuyoshi, "On the Law of Misture of Creep Strength of Fiber Reinforced Composite Materials," Symposium on Structures, jointly sponsored by Japan Society for Aeronautical and Space Sciences and Japan Society for Mechanical Engineers, Tokyo: July 8, 1967.

5. Ellison, E. G., and Landes, J. D., "Creep Analysis for Composite Member," ASME Metals Engineering Conference. Houston, Texas: April 3-5, 1967, Paper 1967 met-16.

6. Antans, V. P., and Skudra, A. M. "Creep of Reinforced Plastics in Uniaxial Tension Along the Fibers," Mekhanika Polimerov, vol. 1, No. 6 (1965), pp. 69-77; rpt. in Polymer Mechanics, Faraday Press, Inc., New York, vol. 1, no. 6 (1968), pp. 41-45.

7. deSilva, A. R. T., "A Theoretical Analysis of Creep in Fiber Reinforced Composites," Journal of the Mechanics and Physics of Solids, vol. 16 (1968), pp. 169-186.

8. Owen, D. R. J., Holbeche, J., Zienkiewicz, O. C., "Elastic and Plastic Analysis of Fiber-Reinforced Materials", Fibre Science Technology, vol. 1 (1969), pp. 185-207.

9. Adams, D. F., "Inelastic Analysis of a Unidirectional Composite Subjected to Transverse Normal Loading," Journal of Composite Materials, vol. 4 (July 1970), pp. 310-328.

10. Isakson, Gabriel, "Descrete-Element Plastic Analysis of Structures in a State of Modified Plane Strain," AIAA Journal, vol. 7, no. 3, (March 1969), pp. 545-547.

11. Greenbaum, G. A., and Rubenstein, M. F., "Creep Analysis of Axisymmetric Bodies Using Finite Elements," Nuclear Engineering and Design, 7(1968), pp. 379-397.

12. Piehler, H. R., "Interior Elastic Stress Field in a Continuous Close-Packed Filamentary Composite Material Under Uniaxial Tension," Fiber-Strengthened Metallic Composites, ASTM STP 427, (1967), pp. 3-26.

13. Garofalo, Frank, Fundamentals of Creep and Creep-Rupture in Metals. New York: Macmillan and Co., 1965.

14. Conway, J. B., Numerical Methods for Creep and Rupture Analysis. New York: Gordon and Breach, 1966.

15. Mendelson, A., Hirschberg, M. H., Manson, S. S., "A General Approach to the Practical Solution of Creep Problems," Journal of Basic Engineering, (Dec. 1959), pp. 585-598.

16. Mendelson, A., Plasticity: Theory and Application, New York: Macmillan and Co., 1968.

17. Sidebottom, O. M., Unpublished data, Theoretical & Applied Mechanics Department, University of Illinois, Urbana, Ill., 1971.

18. Branca, T. R., "Creep of an Uniaxial Metal Matrix Composite Subjected to Axial and Normal Lateral Loads," Thesis, Theoretical & Applied Mechanics Department, University of Illinois, Urbana, Ill., 1971.

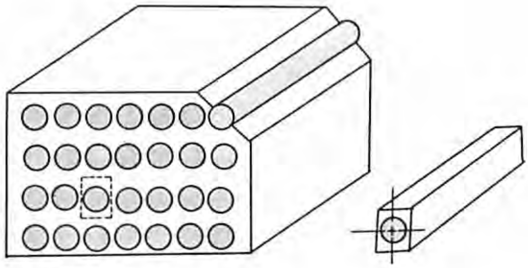

Fig. 1 Composite Cross-Section with Repeating Unit or Cell.

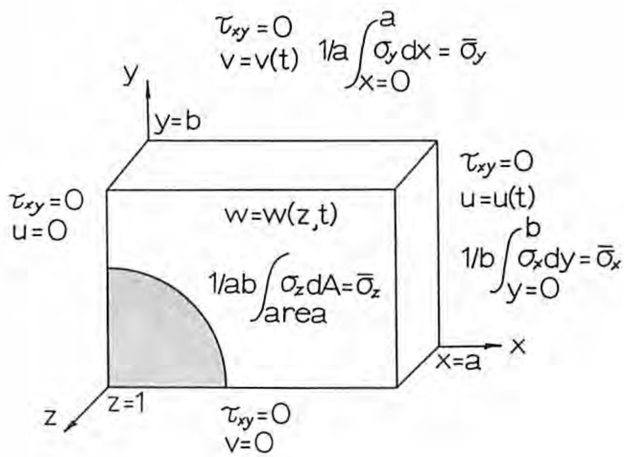

Fig. 2 Boundary Conditions on Composite Repeating Unit.

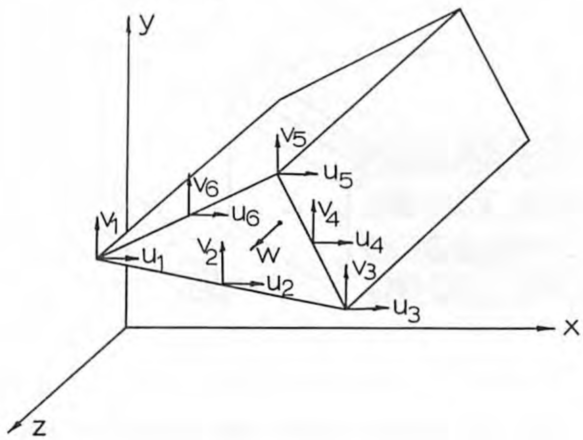

Fig. 3 Element for Finite Element Analysis.

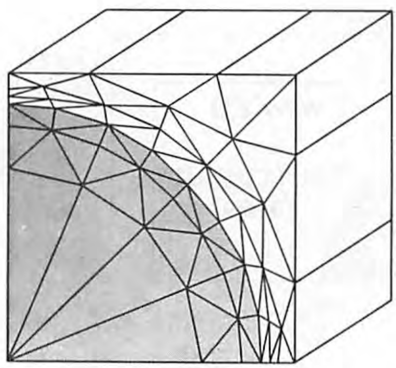

Fig. 4 Finite Element Idealization of Composite Unit, Volume of Fiber, V_f = 62.1%.

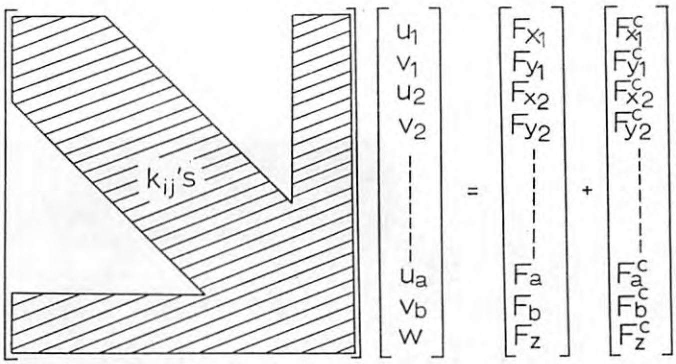

Fig. 5 Schematic of Equations of the Finite Element Formulation.

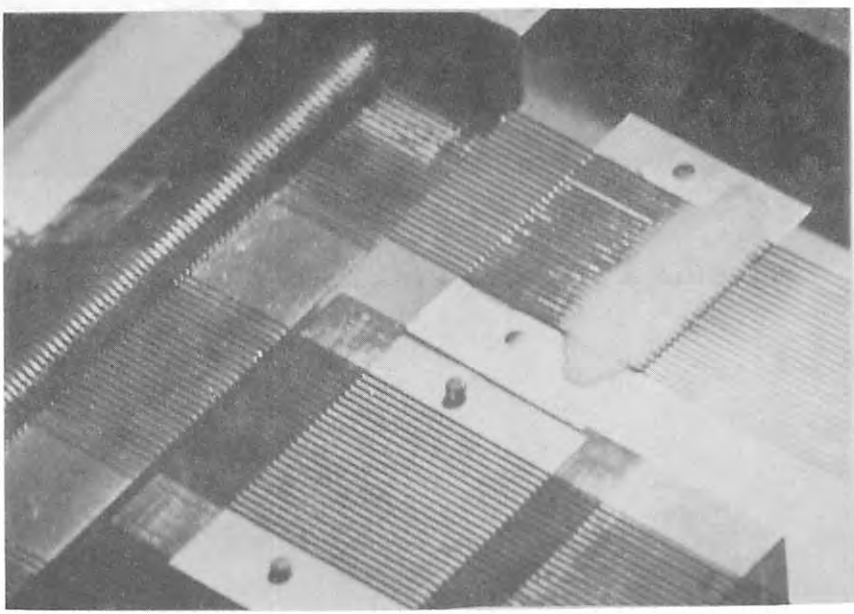

Fig. 6 Positioning and Cementing of Copper Wires to Shim Stock Tabs.

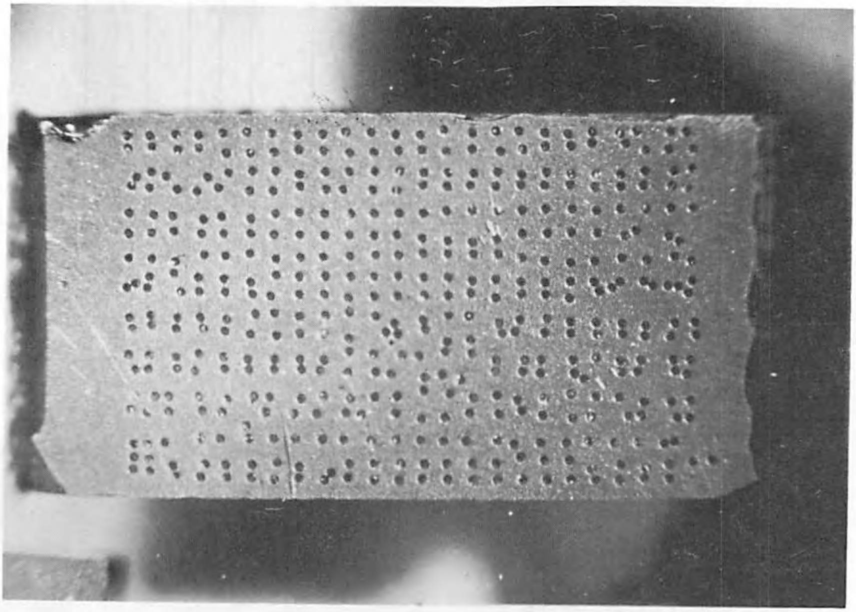

Fig. 7 Cross-Section of Composite, Copper Wires in Lead-Tin Alloy Matrix, V_f = 14.2%.

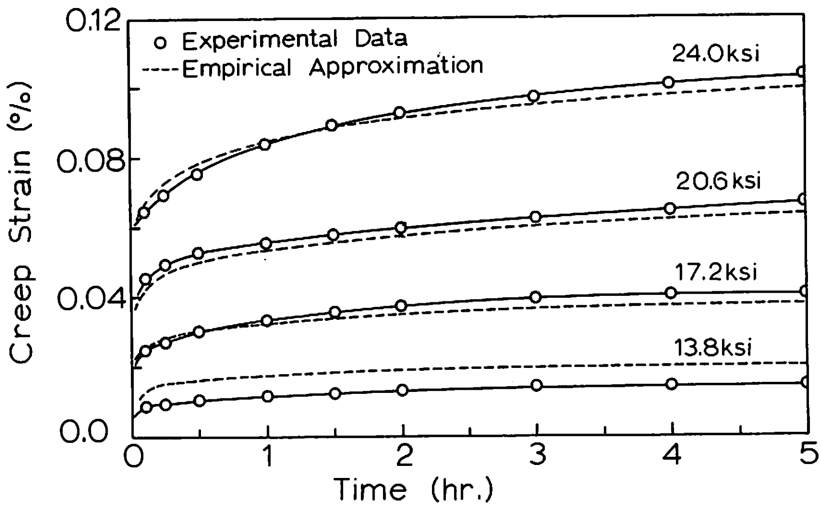

Fig. 8 Room Temperature Creep of Copper Wire.

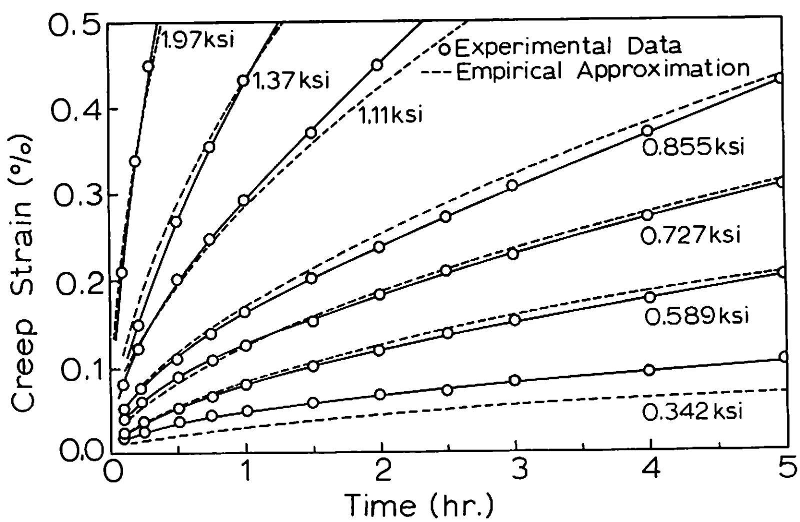

Fig. 9 Room Temperature Creep of Pb-Sn Matrix Alloy.

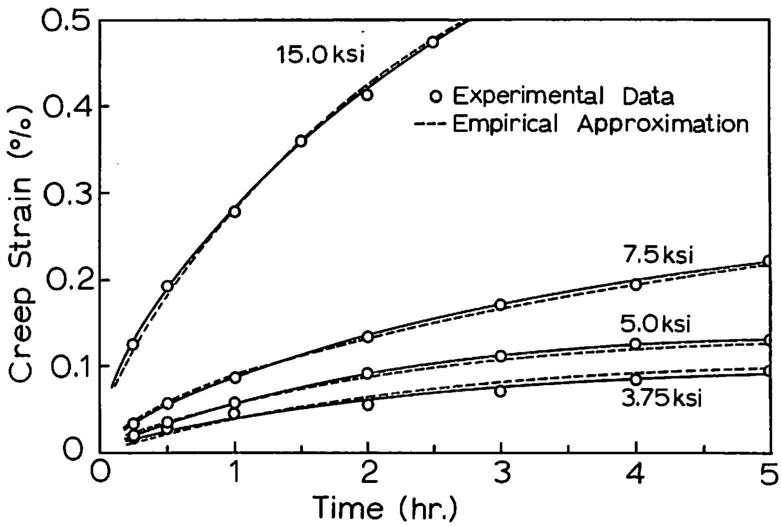

Fig. 10 Creep of Ti 6Al-4V at 1000°F.

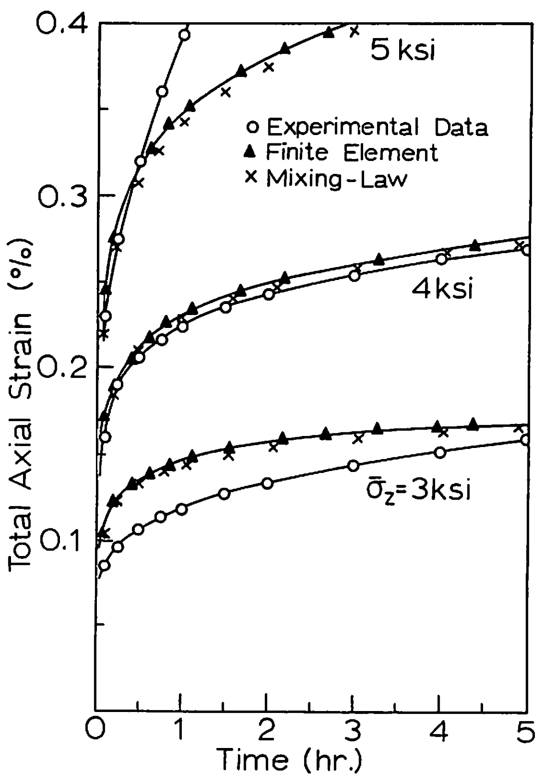

Fig. 11 Axial Creep of Cu-(Pb-Sn) Composite, V_f = 14.2%, $\bar{\sigma}_x = \bar{\sigma}_y = 0$, Room Temperature.

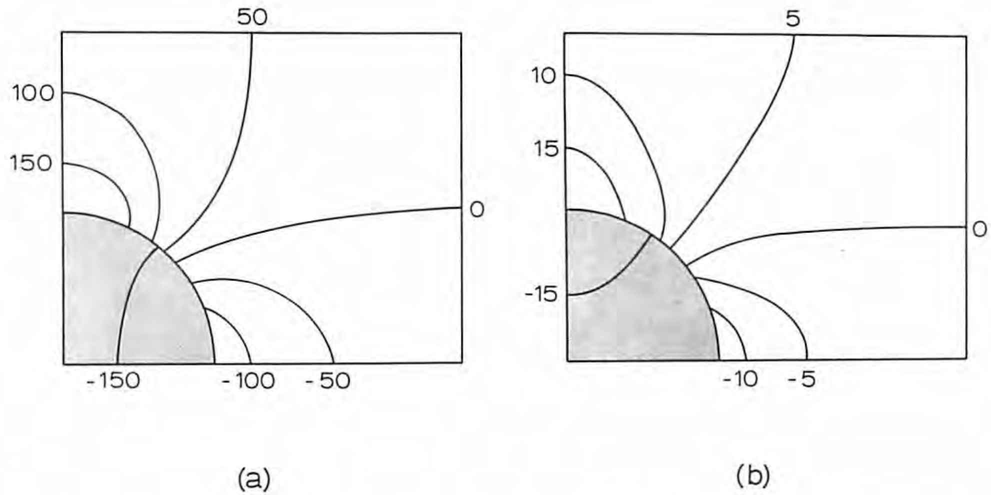

Fig. 12 Component of Lateral Stress σ_x (psi) Cu-(Pb-Sn) Composite, V_f = 14.2%, σ_z = 4ksi, $\bar{\sigma}_x = \bar{\sigma}_y = 0$, Room Temperature, (a)Elastic Solution,(b)After 1.7 hr. of test.

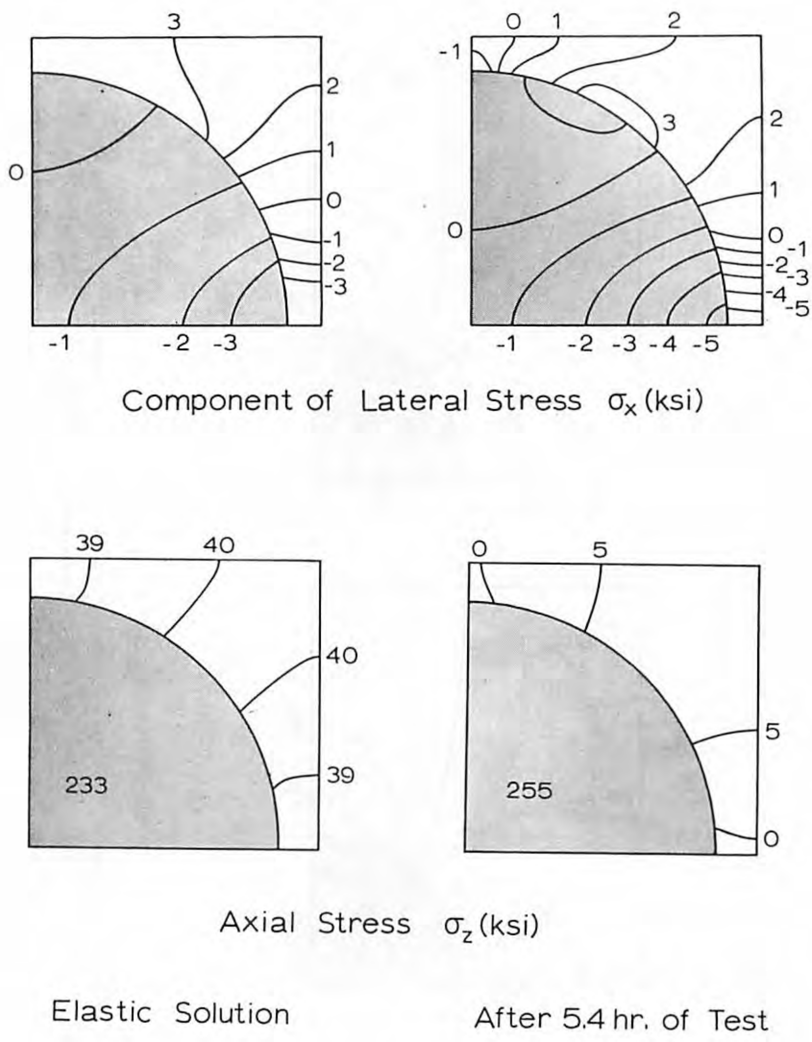

Fig. 13 SiC-Ti Composite, V_f = 62.1%, $\overline{\sigma}_z$ =160 ksi, $\overline{\sigma}_x = \overline{\sigma}_y = 0$, T = 1000°F.

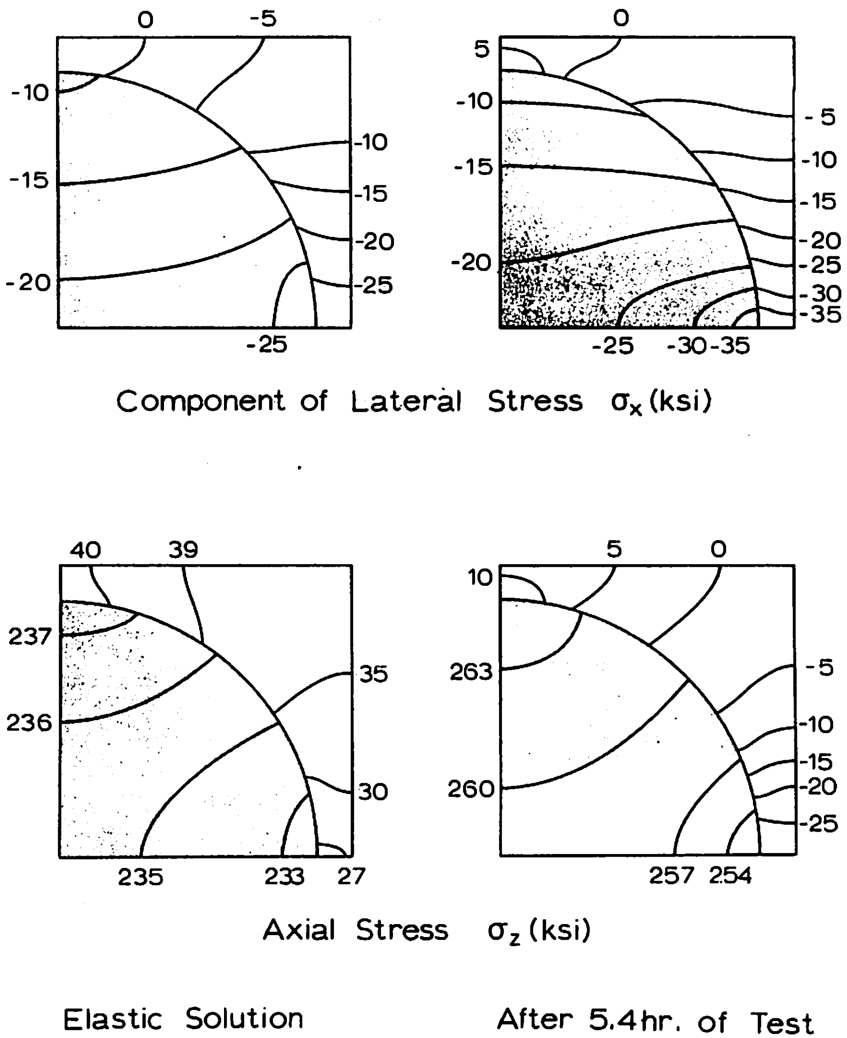

Fig. 14 SiC-Ti Composite, V_f = 62.1%, $\overline{\sigma}_z$ = 160 ksi, $\overline{\sigma}_x$ = -15 ksi, $\overline{\sigma}_y$ = 0, T = 1000°F.

DISCUSSION

Q A. PHILLIPS, U. S. A.

It is not surprising that there is a discrepancy between theory and experiment, since we do not know much about the material behaviour. I suggest that additional experimental work should be directed towards learning more about the material behaviour.

A A. P. BORESI, U. S. A.

I agree. The simple objective we had here, was to compute the interaction of fiber and matrix with presently known material properties. However, at Illinois we have a program in which more complete studies of composite materials are being conducted.

Q R. W. WEEKS, U. S. A.

Did you attempt to analyze the behaviour of the composite under variable loading histories or only for constant loading ?

A A. P. BORESI, U. S. A.

Not in this particlar paper. However, we have started a program in which stepped loading will be considered.

Q R. K. PENNY, U. K.

Could you say more about the one-dimensional mixing law ?

A A. P. BORESI, U. S. A.

Yes. The mixing law is a proportional of load carrying capabilities of fiber and matrix by volume content, much as is done in ultimate strength calculations in reinforced concrete.

Q E. Y. W. TSUI, U. S. A.

In the resulting matrix formulation, there are coupling terms in addition of the banded diagonal matrix, as illustrated by the vertical and horizontal branches of the K_{ij}'s. Would you comment on the causes which produce these coupling terms ?

A A. P. BORESI, U. S. A.

Yes. These terms come from the displacement boundary conditions on the lateral forces of the element and the axial displacement constraint. The axial displacements enter into all elements of the finite element model. The lateral displacements enter into finite elements on the lateral surface. The result is a set of three equations which result in the horizontal and vertical branches of the stiffness matrix.

Q

D. G. HAVARD, Canada

Would the authors please clarify their assumptions regarding the variation of Poisson's ratios of their materials with stress level.

A

A. P. BORESI, U. S. A.

The elastic value of Poisson's ratio was maintained constant for each component material. For the inelastic part of the strain, Poisson's ratio was effectively taken to be 0.50.